

Optical study on the spin-density wave properties in single crystalline  $\text{Na}_{1-x}\text{FeAs}$ 

W. Z. Hu, G. Li, P. Zheng, G. F. Chen, J. L. Luo, and N. L. Wang  
 Beijing National Laboratory for Condensed Matter Physics,  
 Institute of Physics, Chinese Academy of Sciences, Beijing 100190, China

We report an optical investigation on the in-plane charge dynamics for  $\text{Na}_{1-x}\text{FeAs}$  single crystal. A clear optical evidence for the spin-density wave (SDW) gap is observed. As the structural/magnetic transitions are separated in the  $\text{Na}_{1-x}\text{FeAs}$  case, we find the SDW gap opens in accordance with the magnetic transition. Comparing with the optical response of other FeAs-based parent compounds, both the gap value  $2\Delta$  and the energy scale for the gap-induced spectral weight redistribution are smaller in  $\text{Na}_{1-x}\text{FeAs}$ . Our findings support the itinerant origin of the antiferromagnetic transition in the FeAs-based system.

PACS numbers: 78.20.-e, 75.30.Fv

The interplay between different instabilities, such as structural distortions, magnetic orderings, and superconductivity, is of central interest in condensed matter physics. The discovery of superconductivity in FeAs-based layered materials<sup>1</sup> offers a new opportunity to study the intriguing interplay between those instabilities. The undoped FeAs-based compounds can only display the structural and magnetic phase transitions, which, depending on materials, could occur either at the same temperature or separately.<sup>2,3,4</sup> The magnetic order has a collinear spin structure with a  $(\pi, 0)$  wavevector in the folded Brillouin zone (two Fe ions per unit cell). Upon electron or hole doping or application of pressure, both the magnetic order and the structural transition are suppressed, and superconductivity emerges.<sup>3,5,6</sup> It is widely believed that the structural distortion is driven by the magnetic transition,<sup>7,8</sup> however, there have been much debate on whether the parent compounds belong to the local or itinerant category of antiferromagnets. One pool of theories invoke an itinerant electron approach to the systems in which the commensurate antiferromagnetic (AFM) order originates from a spin-density wave (SDW) instability due to the nesting of the electron and hole Fermi surfaces which are separated by a  $(\pi, 0)$  wavevector.<sup>9,10,11,12,13</sup> The itinerant electrons and holes are removed by the gapping of the Fermi surface (FS) in the SDW ordered state. Alternatively, a Heisenberg magnetic exchange model is suggested to explain the AFM structure.<sup>7,8,14,15,16</sup> In this picture, the AFM order is a signature of local physics. On the other hand, Igor Mazin recently argued that neither the itinerant nor the local moment pictures are fully correct. The moments are largely local, driven by the Hund's coupling rather than by the on-site Hubbard repulsion, while the ordering is driven mostly by the gain of the one-electron energies of all occupied states.<sup>17</sup>

The advantage for spectroscopic techniques is detecting the energy gap in the broken symmetry state. Previous optical investigations provide clear evidence for the formation of the SDW partial gap in the magnetic phase in polycrystalline  $\text{ReFeAsO}$  ( $\text{Re} = \text{La}, \text{Ce}, \text{Nd}, \text{etc}$ )<sup>9,18,19,20</sup> and single crystalline  $\text{AFe}_2\text{As}_2$  ( $\text{A} = \text{Ba}, \text{Sr}$ )<sup>21,22</sup> which, therefore, support the itinerant picture

that the energy gain for the AFM ground state is achieved by the opening of an SDW gap on the Fermi surface. Quantum oscillation experiment revealed three Fermi surfaces with area much smaller than those in the paramagnetic phase predicted by the local density approximation calculation,<sup>23</sup> thus agree with optical observation of a large reduction of effective carrier density in the SDW state. However, angle-resolved photoemission spectroscopy (ARPES) experiments did not yield consistent results.<sup>24,25,26,27</sup> On the other hand, the iron chalcogen-based parent compound,  $\text{Fe}_{1-x}\text{Te}$ , which also exhibits structural and magnetic phase transition near 65 K, shows no signature of gap opening for the magnetic ordered state from infrared spectroscopy measurement.<sup>28</sup> As neutron experiments revealed that the low-T magnetic phase has a bi-collinear spin structure with a  $(\pi, 0)$  wavevector,<sup>29,30</sup> which is different from the  $(\pi, \pi)$  wavevector that connects the electron and hole pockets, the absence of gap opening below  $T_{\text{SDW}}$  is not surprising. Anyhow, further spectroscopic studies are required to find out whether the gap formation is a common feature for different types of Fe-based parent compounds. A rather important question is whether the gap emerges after the structural distortion or below the magnetic transition. As the magnetic and structural transitions occur simultaneously in  $\text{AFe}_2\text{As}_2$  (122-type), while no single crystal with sufficient size for optical measurement is obtained for  $\text{ReFeAsO}$  (1111-type), finding a new type of FeAs-based parent compound with well-separated structural/magnetic transitions from which sizeable single crystals can be easily obtained is highly required.

Recently, high quality single crystals are synthesized for almost stoichiometric  $\text{Na}_{1-x}\text{FeAs}$ , a 111-type FeAs-based parent compound. Two separated structural/magnetic transitions at 52 and 41 K, together with a superconducting transition at 23 K are found by transport measurements.<sup>31</sup> Here we report the in-plane optical properties for  $\text{Na}_{1-x}\text{FeAs}$  single crystal. Clear optical evidence for the SDW gap is found, and the gap emerges in accordance with the magnetic transition. Moreover, the gap value  $2\Delta$  has a smaller energy scale than 122-type compounds with higher SDW transition temperatures. The ratio of  $2\Delta/k_B T_{\text{SDW}} \approx 4.2$  is close to the

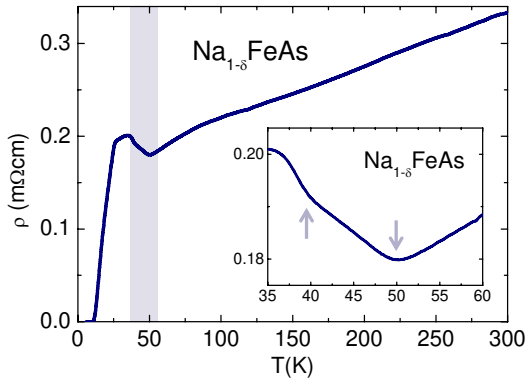


FIG. 1: The in-plane dc resistivity for  $\text{Na}_{1-x}\text{FeAs}$  single crystal. Two separated transitions around 40 and 50 K can be better resolved in the inset figure.

expectation of mean field theory for an itinerant SDW order. Like the 122 systems, a residual Drupe term (free-carrier response) is seen in the SDW ordered phase, thus  $\text{Na}_{1-x}\text{FeAs}$  is still metallic when the SDW gap develops. Then, metallic response and the SDW gap appear to be a common feature for the undoped FeAs-based materials.

Single crystalline  $\text{Na}_{1-x}\text{FeAs}$  samples were grown by the self-flux method.<sup>31</sup> The obtained crystals can be easily cleaved along ab-plane. The dc resistivity ( $\rho$ ) is obtained by the standard four-probe method on a sample cleaved from the same crystal used in the optical measurement. The result is shown in Fig.1. Two transitions near 40 and 50 K were assigned to separated structural and magnetic transitions,<sup>31</sup> which were confirmed by recent neutron diffraction measurement.<sup>32</sup> Here the dc resistivity turns up after the structural distortion, and increases more rapidly with decreasing  $T$  in the SDW state. A superconducting transition is seen with an onset temperature of 25 K, and a zero resistivity is approached when  $T \approx 10$  K. This was interpreted as due to the slight Na deficiency (less than 1%). Since no detectable specific heat anomaly around  $T_c$  was found, the superconducting volume fraction is rather small.<sup>31</sup> We expect that the optical data are dominated by the response of the parent phase.

The optical reflectance measurements were performed on a combination of Bruker IFS 66v/s and 113v spectrometers on newly cleaved surfaces (ab-plane) in the frequency range from 40 to 25000  $\text{cm}^{-1}$ . An in situ gold and aluminum overcoating technique was used to get the reflectivity  $R(\omega)$ . The real part of conductivity  $\sigma_1(\omega)$  is obtained by the Kramers-Kronig transformation of  $R(\omega)$ .

Figure 2 shows the room-temperature optical reflectivity and conductivity spectra over broad frequencies up to 25000  $\text{cm}^{-1}$ . The overall spectral line shapes are very similar to the  $\text{AFe}_2\text{As}_2$  ( $\text{A} = \text{Ba}, \text{Sr}$ ) single crystals. As a comparison, we have included the optical data on  $\text{BaFe}_2\text{As}_2$  in the figure.<sup>21</sup> The reflectance drops almost linearly with frequency at low- $\omega$  region, then merges into the high values of a background contributed mostly from

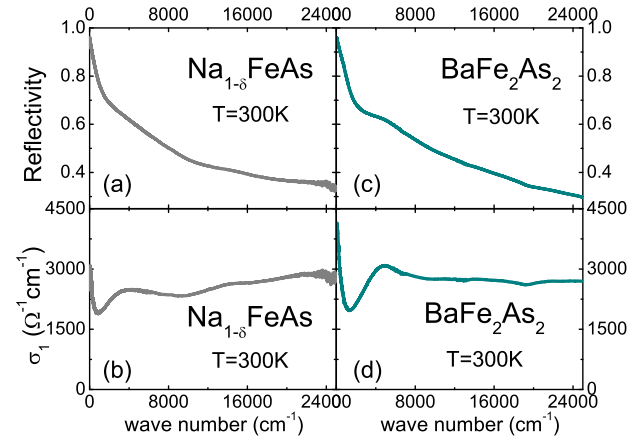


FIG. 2: The room-temperature optical reflectivity (a) and conductivity (b) for  $\text{Na}_{1-x}\text{FeAs}$  single crystal over broad frequencies up to 25000  $\text{cm}^{-1}$ . The optical data on  $\text{BaFe}_2\text{As}_2$  crystal<sup>21</sup> in the same frequency range are shown in (c) and (d) for comparison.

the interband transitions from the mid-infrared to visible regime. By fitting the conductivity spectrum with the Drupe and Lorentz model in a way similar to what we did for 122-type crystals,<sup>21</sup> we get the plasma frequency  $\omega_p \approx 10200$   $\text{cm}^{-1}$  and scattering rate  $\Gamma = 650$   $\text{cm}^{-1}$  for  $\text{Na}_{1-x}\text{FeAs}$ . Both are comparable to the parameters found for the 122-type materials.<sup>21,22</sup> This indicates that we are measuring the charge dynamics of  $\text{Fe}_2\text{As}_2$  layers.

Figure 3 shows the optical reflectivity  $R(\omega)$  for  $\text{Na}_{1-x}\text{FeAs}$  below 600  $\text{cm}^{-1}$ . Two phonons around 160 and 244  $\text{cm}^{-1}$  can be found.  $R(\omega)$  at low  $T$  decreases gradually below 400  $\text{cm}^{-1}$ , consists with the increasing of  $\rho(T)$  below 50 K. In the SDW state, a suppression in

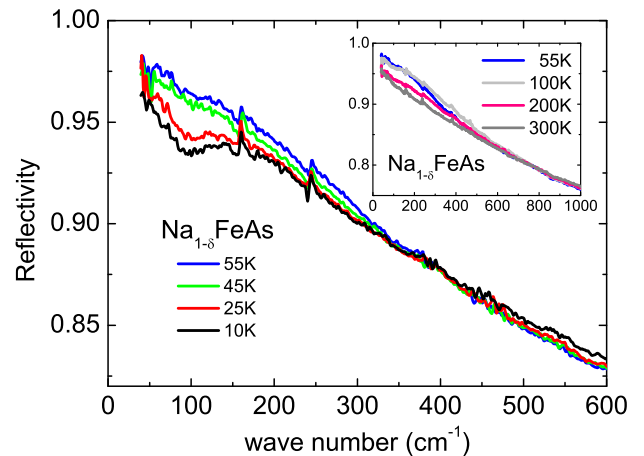


FIG. 3: (Color online) Optical reflectivity  $R(\omega)$  for  $\text{Na}_{1-x}\text{FeAs}$  single crystal. The main figure shows  $R(\omega)$  below 600  $\text{cm}^{-1}$  for  $T = 55$  K. The SDW gap is evidenced by a spectral suppression in the far-infrared for  $T = 10$  and 25 K. The inset plots  $R(\omega)$  below 1000  $\text{cm}^{-1}$  for 55, 100, 200 and 300 K.

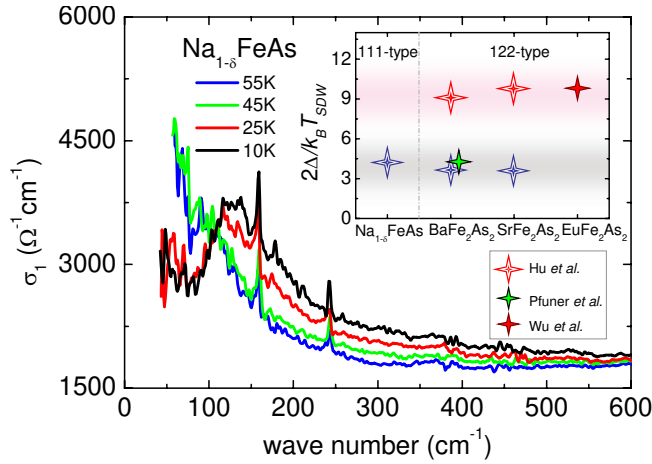


FIG. 4: (Color online) The real part of optical conductivity  $\sigma_1(\omega)$  for  $\text{Na}_{1-x}\text{FeAs}$  below  $600 \text{ cm}^{-1}$ . A SDW gap feature emerges for  $T < T_{\text{SDW}}$ . Inset:  $2\Delta/k_B T_{\text{SDW}}$  obtained from optical data for various single crystalline FeAs-based parent compounds, including  $\text{Na}_{1-x}\text{FeAs}$  (this study),  $\text{BaFe}_2\text{As}_2$  (Hu et al.<sup>21</sup>, Pfüner et al.<sup>33</sup>),  $\text{SrFe}_2\text{As}_2$  (Hu et al.<sup>21</sup>), and  $\text{EuFe}_2\text{As}_2$  (Wu et al.<sup>22</sup>).

$\sigma_1(\omega)$  below  $150 \text{ cm}^{-1}$  is observed, indicating the opening of an SDW gap on the Fermi surface. Similar cases were found for the undoped 122-type<sup>21,22,33</sup> and 1111-type<sup>19,20</sup> compounds. Here the suppression exists only for  $T = 10$  and  $25 \text{ K}$ , while no clear indication for the gap is seen at  $T = 45 \text{ K}$  when the sample just experiences a structural distortion but without any magnetic ordering. The inset plots the low frequency  $\sigma_1(\omega)$  for  $T = 55, 100, 200$  and  $300 \text{ K}$ . Here  $\sigma_1(\omega)$  shows a metallic response in the far-infrared region, that the reactivity continues to grow with lowering  $T$  in the normal state, in agreement with the metallic response as seen in the dc resistivity.

The low- $\omega$  temperature-dependent real part of conductivity  $\sigma_1(\omega)$  is shown in Fig. 4. Besides two sharp phonon modes around  $160$  and  $244 \text{ cm}^{-1}$ ,  $\sigma_1(\omega)$  for both  $T = 45$  and  $55 \text{ K}$  show a Drude response without any clear evidence for the gap-induced absorption peak. For  $T = 10$  and  $25 \text{ K}$ , a peak with a clear edge-like feature is formed around  $120 \text{ cm}^{-1}$ . Therefore, the energy gap emerges only in the antiferromagnetic state. Meanwhile, a remaining Drude component is seen below  $80 \text{ cm}^{-1}$ , indicating that the Fermi surface is only partially gapped and  $\text{Na}_{1-x}\text{FeAs}$  is still metallic in the SDW state. In our earlier study on  $\text{AFe}_2\text{As}_2$  ( $\text{A} = \text{Ba}, \text{Sr}$ ) single crystals, we know that the residual Drude component in the SDW state has a much smaller spectral weight and a narrower peak width, indicating the removal of both conducting carriers and the scattering channel.<sup>21</sup> Here, essentially we see the same structural feature. However, because of the limited frequency range below the energy gap, a quantitative estimation for the loss of carrier density and scattering rate could not be accurately determined.

The optical conductivity  $\sigma_1(\omega)$  shows different gap characters for the superconducting and the density wave

states due to their respective coherence factors.<sup>34,35</sup> For the SDW ground state with an isotropic gap, a non-symmetric peak with clear edge-like feature emerges at  $2\omega$  in the optical conductivity, so that  $\sigma_1^{\text{SDW}}(\omega)$  exceeds the normal state conductivity  $\sigma_1^{\text{N}}(\omega)$  at the gap onset,<sup>34</sup> above which the loss in free-carrier (Drude) spectral weight is gradually compensated by the gap-induced absorption peak. For a multi-band system, gap anisotropy will weaken the edge-like feature at  $2\omega$ . Here we use the peak position (the conductivity maximum) to estimate the SDW gap. For  $\text{Na}_{1-x}\text{FeAs}$ , the conductivity peak at  $10 \text{ K}$  is around  $120 \text{ cm}^{-1}$ , i.e.,  $2\omega_{\text{SDW}} \approx 15 \text{ meV}$ . Such a gap is obviously smaller than that in  $\text{AFe}_2\text{As}_2$  and  $\text{ReFeAsO}$ .<sup>19,20,21,22,33</sup>

In undoped 122-type compounds  $\text{AFe}_2\text{As}_2$ , ( $\text{A} = \text{Sr}, \text{Ba}, \text{Eu}$ ), a double-gap character is found with the  $2\omega/k_B T_{\text{SDW}} \approx 9$  and  $4$ , respectively. For  $\text{Na}_{1-x}\text{FeAs}$ , only one energy gap feature is observed in the measurement frequency range with  $2\omega/k_B T_{\text{SDW}} \approx 4.2$ . From the spectral lineshape, this gap feature should correspond to the higher energy gap feature in undoped 122 compounds. It is not clear whether a second feature at lower energy scale exists beyond the lowest measurement energy. Thus, although qualitatively the energy gaps are smaller for undoped compounds with lower SDW transition temperatures, there is no scaling relation between different compounds with different  $T_{\text{SDW}}$ . In the inset of Fig. 4 we show  $2\omega/k_B T_{\text{SDW}}$  obtained by optical data on 111 ( $\text{Na}_{1-x}\text{FeAs}$ ) and 122 ( $\text{AFe}_2\text{As}_2$ ,  $\text{A} = \text{Sr}, \text{Ba}, \text{Eu}$ )<sup>21,22,33</sup> type parent compounds. Here the gap  $2\omega$  for different FeAs systems are all defined by the peak positions in  $\sigma_1(\omega)$  for consistency.

Besides the gap value, the energy scale affected by the SDW gap is also smaller for  $\text{Na}_{1-x}\text{FeAs}$  in comparison with other FeAs-based parent compounds with higher  $T_{\text{SDW}}$ s. Figure 5 plots the spectral weight at  $10$  and  $45 \text{ K}$  for  $\text{Na}_{1-x}\text{FeAs}$ . The inset shows the spectral weight at  $T = 100, 200$  and  $300 \text{ K}$ . Note  $\text{Na}_{1-x}\text{FeAs}$  is metallic in the normal state (Fig. 1), so the spectral weight piles up

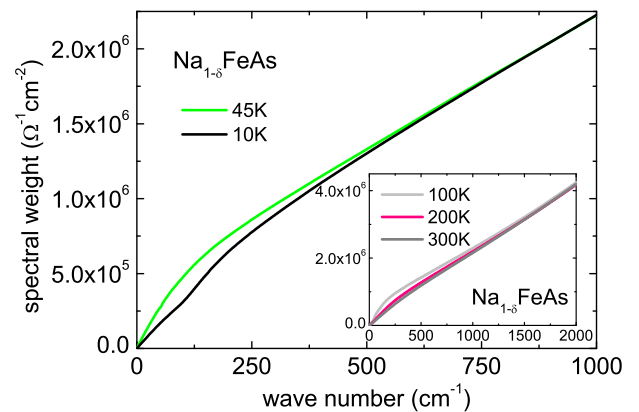


FIG. 5: (Color online) The spectral weight  $\int_0^{\omega} \sigma_1(\omega') d\omega'$  for  $\text{Na}_{1-x}\text{FeAs}$  below  $1000 \text{ cm}^{-1}$  for  $T = 10$  and  $45 \text{ K}$ . Inset: the spectral weight for  $T = 100, 200$ , and  $300 \text{ K}$  up to  $2000 \text{ cm}^{-1}$ .

at low frequencies with decreasing  $T$ , which is due to an increasing dc conductivity ( $\sigma_1(0)$ ) thus a growing Drude peak in  $\sigma_1(\omega)$ . Above  $1700 \text{ cm}^{-1}$ , the spectral weight for all temperatures merge together. In the SDW state, the spectral weight is smaller for 10 K than that of 45 K, indicating a loss in the Drude weight at 10 K, that part of the free carriers are removed from  $E_F$  due to the SDW gap. The spectral weight loss in low frequencies is compensated when  $\omega$  approaches  $750 \text{ cm}^{-1}$ . Such an energy scale is smaller than that of  $\text{AFe}_2\text{As}_2$  (e.g.  $2000 \text{ cm}^{-1}$  for  $\text{BaFe}_2\text{As}_2$  where  $T_{\text{SDW}} \approx 140 \text{ K}$ ).<sup>21</sup>

Our study clearly indicates that the metallic response and the opening of an energy gap in the magnetic ordered state are ubiquitous behaviors for all FeAs-based undoped compounds. In addition, the gap magnitude correlates with  $T_{\text{SDW}}$ . Associated with the gapping of the Fermi surface, a large part of the Drude component is removed (indicating a reduction of the FS area) and the scattering channel is also reduced. All favor an itinerant origin of the SDW order. We noticed that some ARPES studies<sup>25,27</sup> on  $\text{BaFe}_2\text{As}_2$  did not reveal any gap in the SDW state, therefore failed to see a dramatic reduction of Fermi surface areas. As the optics probes the bulk properties, while the ARPES is mainly a surface probe, it remains to clarify if there is a surface reconstruction which would affect the results. Considering the multiband/orbital character for FeAs-based compounds, the entire band structure might be reconstructed when parts of them were modified by FS nesting instability. In

this sense, our optical data do not conflict with the band reconstruction picture.

Finally, we comment on the upturn behavior of the dc resistivity below the structural/magnetic phase transition. Note ( $T$ ) turns up for  $\text{Na}_1\text{FeAs}$  but drops more steeply with decreasing  $T$  for  $\text{AFe}_2\text{As}_2$  and  $\text{ReFeAsO}$ . From the semi-classic Boltzmann transport theory, the resistivity is determined by the complex function of Fermi velocity, the scattering rate, and their weighted integral over the whole FS.<sup>36</sup> In the case of electron gas, it could be simplified to the Drude form for which the resistivity is determined by carrier density and scattering rate. So apparently, whether shows an upturn or a fast drop depends on the subtle balance of those quantities which experience substantial changes across the transition.

To summarize, we studied the in-plane optical properties for  $\text{Na}_1\text{FeAs}$ , a FeAs-based parent compound with separated structural and magnetic transitions. It shares similar optical response over broad frequencies with other FeAs-based systems. A clear energy gap in  $\sigma_1(\omega)$  is observed below the magnetic phase transition, accompanied by a spectral weight transfer from the free-carrier Drude term to above this gap energy. Both the gap  $\Delta$  and the energy scale associated with the spectral weight redistribution are smaller in comparison with other undoped FeAs-based compounds with higher  $T_{\text{SDW}}$ . The results favor an itinerant origin for the SDW transition.

This work is supported by the NSFC, CAS, and the 973 project of the MOST of China.

- 
- <sup>1</sup> Y. Kamihara, T. Watanabe, M. Hirano, and H. Hosono, *J. Am. Chem. Soc.* **130**, 3296 (2008).
- <sup>2</sup> C. Larina de la Cruz, Q. Huang, J. W. Lynn, Jiying Li, W. Ratcli II, J. L. Zarestky, H. A. Mook, G. F. Chen, J. L. Luo, N. L. Wang, and Pengcheng Dai, *Nature* **453**, 899 (2008).
- <sup>3</sup> M. Rotter, M. Tegel, D. Johrendt, *Phys. Rev. Lett.* **101**, 107006 (2008).
- <sup>4</sup> J. H. Chu, J. G. Analytis, C. Kucharczyk, and I. R. Fisher, *Phys. Rev. B* **79** 014506 (2009).
- <sup>5</sup> Jun Zhao, Q. Huang, C. Larina de la Cruz, Shiliang Li, J. W. Lynn, Y. Chen, M. A. Green, G. F. Chen, G. Li, Z. Li, J. L. Luo, N. L. Wang, Pengcheng Dai, *Nature Materials* **7**, 953 (2008).
- <sup>6</sup> M. S. Torikachvili, S. L. Bud'ko, N. Ni, P. C. Canfield, *Phys. Rev. Lett.* **101**, 057006 (2008).
- <sup>7</sup> T. Yildirim, *Phys. Rev. Lett.* **101**, 057010 (2008).
- <sup>8</sup> C. Fang, H. Yao, W.-F. Tsai, J. P. Hu, S. A. Kivelson, *Phys. Rev. B* **77**, 224509 (2008); C. Xu, M. Muehler, S. Sachdev, *Phys. Rev. B* **78**, 020501(R) (2008).
- <sup>9</sup> J. Dong, H. J. Zhang, G. Xu, Z. Li, G. Li, W. Z. Hu, D. Wu, G. F. Chen, X. Dai, J. L. Luo, Z. Fang, N. L. Wang, *Europhys. Lett.* **83**, 27006 (2008).
- <sup>10</sup> I. I. Mazin, D. J. Singh, M. D. Johannes, M. H. Du, *Phys. Rev. Lett.* **101**, 057003 (2008).
- <sup>11</sup> Ying Ran, Fa Wang, Hui Zhai, Ashvin Vishwanath, Donghai Lee, *Phys. Rev. B* **79**, 014505 (2009).
- <sup>12</sup> V. Cvetkovic and Z. Tesanovic, *European Physics Letters* **85**, 37002 (2009).
- <sup>13</sup> D. J. Singh, *Physica C* **469**, 418 (2009) and references therein.
- <sup>14</sup> Q. Si and E. Abrahams, *Phys. Rev. Lett.* **101**, 076401 (2008).
- <sup>15</sup> F. J. Ma, Z. Y. Lu, and T. Xiang, *Phys. Rev. B* **78**, 224517 (2008).
- <sup>16</sup> J. Wu, P. Phillips and A. H. Castro Neto, *Phys. Rev. Lett.* **101**, 126401 (2008).
- <sup>17</sup> M. D. Johannes and I. I. Mazin, *Phys. Rev. B* **79**, 220510(R) (2009).
- <sup>18</sup> G. F. Chen, Z. Li, D. Wu, G. Li, W. Z. Hu, J. Dong, P. Zheng, J. L. Luo, and N. L. Wang, *Phys. Rev. Lett.* **100**, 247002 (2008).
- <sup>19</sup> W. Z. Hu, Q. M. Zhang, and N. L. Wang, *Physica C* **469**, 545 (2009).
- <sup>20</sup> A. V. Boris, N. N. Kovaleva, S. S. A. Seo, J. S. Kim, P. Popovich, Y. Matsui, R. K. Kramers, and B. Keimer, *Phys. Rev. Lett.* **102**, 027001 (2009).
- <sup>21</sup> W. Z. Hu, J. Dong, G. Li, Z. Li, P. Zheng, G. F. Chen, J. L. Luo, and N. L. Wang, *Phys. Rev. Lett.* **101**, 257005 (2008).
- <sup>22</sup> D. Wu, N. Barisic, N. D. Richko, S. Kaiser, A. Faridian, M. Dressel, S. Jiang, Z. Ren, L. J. Li, G. H. Cao, Z. A. Xu, H. S. Jeevan and P. G. Egenwart, *Phys. Rev. B* **79**, 155103 (2009).
- <sup>23</sup> Suchitra E. Sebastian, J. Gillett, N. Harrison, P. H. C. Lau, D. J. Singh, C. H. Mielke and G. G. Lonzarich, *J. Phys.: Condens. Matter* **20**, 422203 (2008).

